

# Behavior of curved steel trapezoidal box-girders during construction

Cem Topkaya, Eric B. Williamson\*, Karl H. Frank

*Department of Civil Engineering, The University of Texas at Austin, Austin, TX 78712, USA*

Received 7 November 2002; received in revised form 12 December 2003; accepted 18 December 2003

## Abstract

In recent years, steel, trapezoidal box-girders for curved highway interchanges have been used extensively. For these structural systems, the majority of the steel girder cross-sectional stresses occur during the concrete pouring sequence. This paper describes a comprehensive study on the behavior of curved girders during construction. Data collected for the current research shows significant differences between the measured and predicted quantities, particularly for later pours. An overview of the steel–concrete interface behavior at early concrete ages and the development of an analytical tool to predict the response of systems with semi-cured concrete are given. Field monitoring of two bridges during construction is presented. The measured results were compared to analytical predictions obtained using software developed specifically under this research to address deficiencies with currently available analytical tools. Accounting for strength and stiffness gained throughout the construction process, the developed software is able to accurately capture girder stresses during construction.

© 2004 Elsevier Ltd. All rights reserved.

*Keywords:* Bridge; Analysis; Field monitoring; Construction; Pour sequence

## 1. Introduction

Due to advances in fabrication technology, the use of steel, trapezoidal box-girders for curved highway interchanges has become popular. The rapid erection, long span capability, economics, and aesthetics of these girders make them more favorable than other structural systems. A typical box-girder system consists of one or more U-shaped steel girders that act compositely with a cast-in-place concrete deck. The composite action between the steel girder and concrete deck is achieved through the use of shear studs welded to the top flanges of the girders (Fig. 1).

The major structural advantage of the trapezoidal box is its large torsional stiffness. A closed box has a torsional stiffness 100–1000 times greater than a comparable I-section [1]. Before hardening of the concrete deck, however, the steel box is an open U-section with very low torsional stiffness and strength. To stabilize the girders during construction and to increase the torsional stiffness prior to hardening of the deck, internal braces are provided. Two different types of internal

bracing systems are used. The first type is a permanent, top-lateral truss system that is used to provide a pseudo-closed section. The second type consists of K or X braces that control stability and cross-sectional distortion (Fig. 1). In addition to internal braces, external diaphragms, which are typically in the form of temporary trusses, are used to minimize distortion between dual or multi-girder systems. External braces are usually removed after the concrete deck hardens for aesthetics and in order to prevent fatigue problems.

Composite box-girders with live loading and the quasi-closed steel box-girders during construction must be evaluated for the design of these bridges. Considering both of these cases, the design for construction loading is the least understood [2] and is the most important. Stresses coming from construction loading can reach up to 60–70% of the total stress on a cross-section [3]. In addition, the forces acting on the bracing members depend almost entirely on the construction loads.

The design for construction loading requires the determination of correct cross-sectional stresses and member forces. Because curved, trapezoidal box-girder bridges have a complex geometry, their analysis presents a great challenge. Several methods exist for

\* Corresponding author. Tel.: +1-512-475-6175.

E-mail address: [ewilliamson@mail.utexas.edu](mailto:ewilliamson@mail.utexas.edu) (E.B. Williamson).

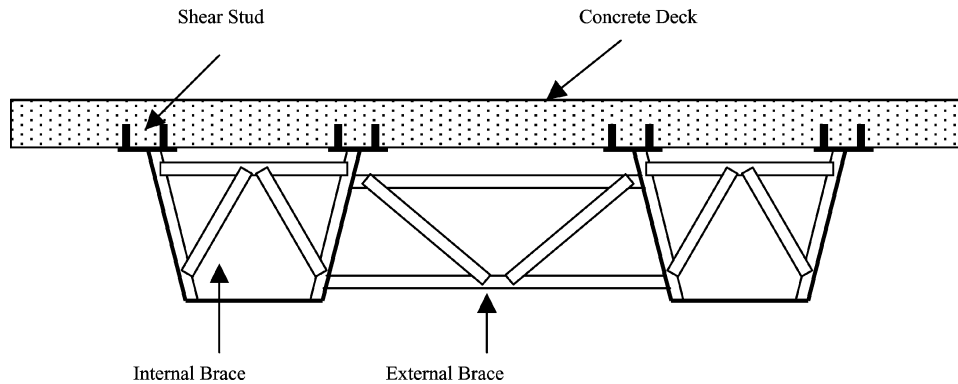


Fig. 1. A typical cross-section of a trapezoidal box-girder system.

analyzing curved box-girders including approximate hand methods, the finite difference method, the finite strip method, the grid analysis method, and the finite element method. Among these, the finite element method (FEM) is the most suitable for construction load analysis. The FEM is capable of modeling a structure in great detail and is more accurate than other methods of analysis. One limitation of this method, however, is that it requires knowledge of advanced analytical methods on the designer's part as well as significant computational resources. In addition, parameter studies with general-purpose FEM software can be difficult because changing the structural layout requires generating a new mesh.

The FEM, just like all other analysis methods, requires the correct mathematical representation of the physical problem being considered. In order to have an accurate model, knowledge of curved box-girder behavior during construction is essential. The majority of the loading during construction comes from the weight of wet concrete. The entire deck is usually not cast in one stage because of the large volume of concrete as well as the need to control shrinkage. Other researchers have monitored these systems during the pouring sequence, and measured data were compared with analysis results obtained from commercially available, sophisticated finite element programs [4,5]. For the later pours in the pouring sequence, significant differences were observed between the measured and predicted quantities. These differences indicated that the girders may become partially composite in sequential stages. Thus, analysis for construction loading should take into account the partial composite action developing between the pouring stages. In order to accurately model these conditions, a thorough understanding of the behavior of both the concrete deck and steel-concrete interface at early ages is required.

Because induced stresses can be large, construction loading should be handled with great care during the design of curved, trapezoidal, steel box-girders. In addition, sophisticated analytical tools are needed to

accurately predict girder response. Lack of knowledge of curved girder behavior and/or use of inadequate analysis tools has resulted in construction failures in the past in which bracing members have buckled [6]. In order to address these issues, a three-phase study was undertaken to investigate the behavior of curved, trapezoidal box-girders during construction. In the first phase, laboratory tests were performed to investigate the shear transfer between the concrete deck and steel girder at early concrete ages. In the second phase, an easy-to-use finite element program was developed for the analysis of these systems under construction loads. The program has the capability of modeling the effects of semi-cured concrete. The third phase focused on the monitoring of two curved, trapezoidal box-girder bridges during construction. In this paper, an overview of the first two phases is given. In addition, details of the field measurements are also presented. The forces and stresses measured in the field are compared with the computed results from analyses with the developed software.

## 2. Overview of shear transfer at early concrete ages

Horizontal shear transfer between a steel girder and concrete deck is typically achieved by using welded headed shear studs. Behavior of shear studs embedded in mature concrete is well documented [7]. Current literature, however, lacks experimental evidence of the behavior of shear studs during early ages of concrete. An experimental program was developed to establish the behavior of the concrete deck-steel girder interface at early concrete ages. In order to investigate the behavior, load-slip curves for the shear studs embedded in early-age concrete were obtained. The current study was limited to one type of concrete mix design typically used for the bridge decks in TX. This mix design is also identical to the one used during the construction of the two curved bridges that were monitored as a part of

this research program. A shear stud diameter of 19 mm (3/4 in.) was used for all specimens.

A total of 24 push-out tests were performed at eight different times varying from 4 h to 28 days after concrete was initially poured. At all time periods, cylinder tests were conducted to determine the compressive and tensile strength and stiffness of concrete. The specimens were air cured inside a laboratory where the ambient temperature was between 30–35 °C (85–95 °F) during the 28-day period. Details of the study on shear transfer at early concrete ages are given in Topkaya [6]. A summary of the findings from the push-out tests [6] is described below.

To quantify the shear stud capacity at early concrete ages, a definition of design strength was proposed. The design strength ( $Q_d$ ) was defined as the value of the load attained at a displacement value of 0.8 mm (0.03 in. (corresponding to diameter/25)). This definition was based on a serviceability limit state which current code equations do not consider. Test results revealed that the design strength is not very sensitive to the slip level in the vicinity of 0.8 mm (0.03 in.). A detailed discussion of the sensitivity of results is given in Topkaya [6]. A summary of the test results for average concrete strength, concrete stiffness, and design strength for shear studs for all time periods is given in Table 1. In addition, the relationship developed to predict the design strength based on concrete properties is given by (Eq.1).

$$\frac{Q_d}{A_{sc}} = 3.8(f'_c E_c)^{0.3} \text{ (SI units)}$$

$$\frac{Q_d}{A_{sc}} = 1.75(f'_c E_c)^{0.3} \text{ (English units)} \quad (1)$$

where  $Q_d$  is design strength (kN),  $A_{sc}$  is cross-sectional area of shear stud ( $\text{mm}^2$ ),  $f'_c$  is compressive strength of concrete (MPa), and  $E_c$  is compressive stiffness of concrete (MPa).

To estimate the shear stud stiffness, a load–slip relationship for the studs was developed. The proposed relationship is given by Eq. (2). This equation gives an initial stiffness of 3.75  $Q_d$  and a secant stiffness at the design load of 1.25  $Q_d$ . The developed load–slip relationship is shown in Fig. 2 together with the initial and final secant stiffness. Because the experimental study was limited to only one stud configuration, this

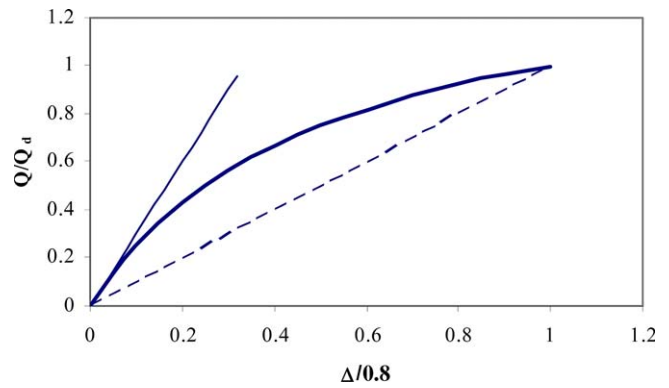


Fig. 2. Load–slip relationship for shear studs with initial and final secant stiffness.

formula may require modification for different stud diameters and configurations.

$$\frac{Q}{Q_d} = \frac{3\left(\frac{\Delta}{0.8}\right)}{1 + 2\left(\frac{\Delta}{0.8}\right)} \quad (2)$$

### 3. Overview of the developed software for pour sequence analysis

Designs of curved-girder systems are usually undertaken by making use of software which is based upon a grid analysis methodology. The grid analysis method requires little computational effort and is fairly easy to implement. Certain assumptions, however, are typically built into the model, especially for systems with quasi-closed cross-sections. For example, the top-lateral bracing system is often approximated as an equivalent plate to calculate the torsional properties of the cross-section. Another drawback with the grid method of analysis is that partial composite action between the steel girder and concrete deck, particularly at early ages, cannot be easily considered. As discussed earlier, during the construction of these curved-girder systems, the concrete deck is poured in a number of stages, and the deck and girder become composite in a time-dependent fashion. Failure to account for this aspect of behavior can lead to inaccurate predictions of brace member forces and stresses in the girder. Also, as

Table 1  
Concrete and stud properties at different times

	Time							
	4 h	8 h	13 h	22 h	3 day	7 day	14 day	28 day
$f'_c$ MPa (psi)	2.19 (318)	5.53 (802)	8.53 (1237)	12.92 (1873)	22.23 (3223)	28.05 (4067)	30.71 (4453)	30.46 (4417)
$E_c$ GPa (ksi)	8.62 (1250)	19.57 (2837)	21.65 (3140)	25.17 (3649)	28.43 (4123)	30.82 (4469)	30.17 (4375)	28.91 (4193)
$Q_d$ kN (kips)	17.2 (3.9)	31.5 (7.1)	39.8 (8.9)	54.0 (12.1)	61.1 (13.7)	66.3 (14.9)	69.5 (15.6)	76.4 (17.2)

indicated previously, the use of inadequate analysis tools have resulted in construction failures in the past [6]. The FEM offers the advantages of both incorporating the effects of semi-cured concrete and modeling the structure in great detail. The main drawbacks of the FEM are that it requires extensive computer resources, and input into the analysis routine can be time consuming. However, with recent advances in hardware and software technology, user-friendly, finite-element-based programs can be developed that reduce some of the limitations that have kept the FEM from being widely used. As such, an easy-to-use software package (UTrAp) has been developed as a part of this research program. An overview of the program is given in the following paragraphs.

UTrAp is capable of analyzing curved, trapezoidal, steel box-girders under construction loads. This program can be readily executed on personal computers. The package consists of an analysis module and a Graphical User Interface (GUI). The analysis module is a linear, three-dimensional finite element program with pre- and post-processing capabilities. The GUI is used to prepare an input file for the analysis module and also to display the results generated by the post-processor. The analysis module itself is capable of generating a finite element mesh, element connectivity data and material properties based on the data supplied through the GUI. The finite element module utilizes nine-node shell elements and two-node truss and spring elements. A constant mesh density is used for all bridges. At a given cross-section, the webs and bottom flanges of the girders are modeled with four shell elements, while two elements are used for top flanges. The concrete deck is modeled with 10 and 20 shell elements for single and dual girder systems, respectively (Fig. 3). Previous work on curved, trapezoidal girders [4] revealed that the mesh density adopted in UTrAp is adequate for the dimensions of most typical cross-sections. Along the length of the bridge, each element is 0.61-m (2-ft) long. Steel sections and the concrete deck are connected together by spring elements that represent the shear studs. Internal, external and top-lateral braces are modeled with truss elements. The types of internal and external bracing configurations that are typically used in practice have been included in the program. For the pour sequence, the concrete deck can be divided into segments along the length of the bridge. For each analysis, properties of the concrete deck can be varied. Concrete modulus, stud stiffness associated with a particular segment, and the distributed load on the segment are the properties required as input. Unlike currently used software for curved girder analysis, UTrAp offers the features of reporting stresses over the cross-section, direct computation of brace forces, and accounting for partially composite cross-section behavior. Currently the program does not include the

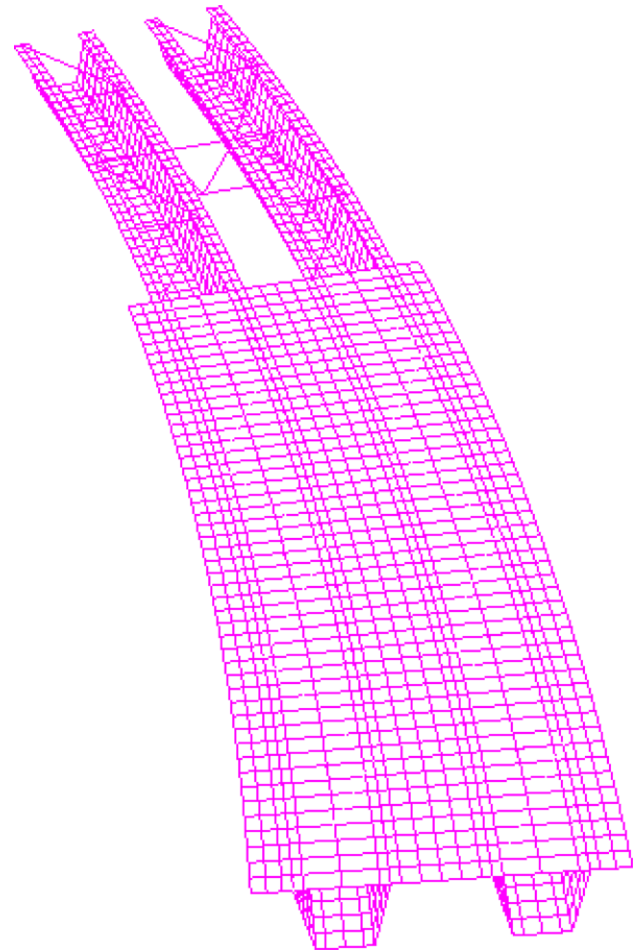


Fig. 3. Portion of a finite element model.

modeling of superelevation, permanent metal deck forms (PMDF), support movements due to flexible bearings, and variable concrete deck thickness profile.

The GUI was designed to provide an environment in which the user easily enters required input data. Cross-sectional dimensions, plate thickness, locations of supports and braces, properties of the concrete deck, and construction loads are input to the program through use of the GUI. In addition, the GUI has the capability of displaying both numerical and graphical output of the analysis results. Deflections, cross-sectional rotation, cross-sectional forces and stresses, and brace member forces can be displayed graphically. Additional details of the computational software are given in Topkaya [6].

## 4. Field studies

### 4.1. Bridges under study

Four trapezoidal, steel, box-girder bridges were constructed at the intersection of IH35 and US290 in Austin,

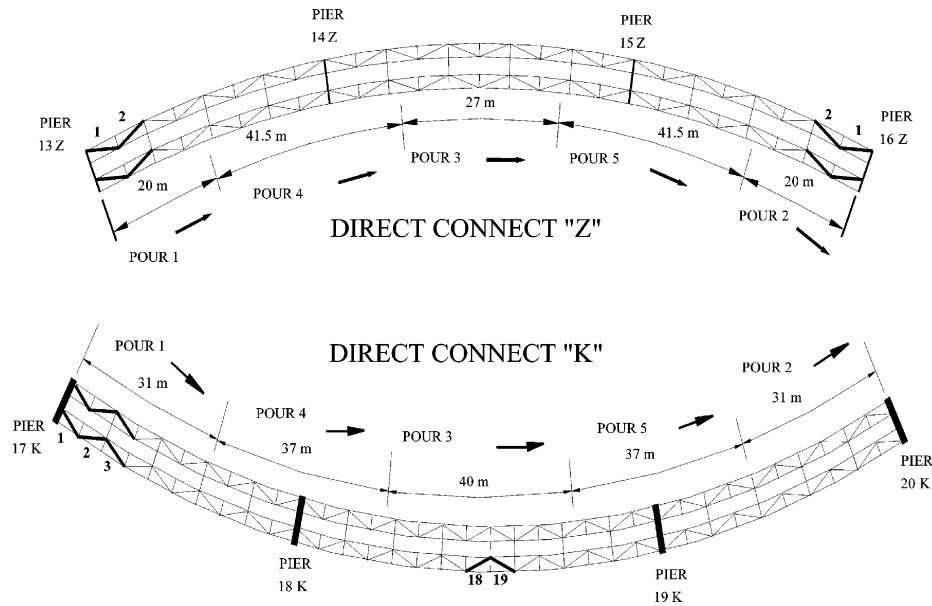


Fig. 4. Plan view of instrumented bridges.

TX. The construction took place between September 1999 and July 2001. Brace members and cross-sectional locations were instrumented for two bridges during construction. The instrumented bridges were called Z- and K-connects. Connect Z consists of one three-span bridge adjacent to a two-span bridge. The three-span portion of the bridge was monitored. The twin-girder symmetrical bridge has two side spans of approximately 46 m (150 ft) in length and a middle span of 58 m (190 ft). The centerline radius of the bridge is 137 m (450 ft).

Connect K is a three-span bridge with two side spans of 51 m (168 ft) and a middle span of 74 m (242 ft). The centerline radius of the bridge is 175 m (573 ft). A plan view of connects Z and K is given in Fig. 4, and the dimensions of the girder cross-sections are shown in Fig. 5. Both connects were supported on elastomeric bearings.

The top and bottom flanges and webs vary in thickness along the length of each of the bridges. Values for the plate thicknesses for both connect Z and connect K are given in Table 2. K-type internal diaphragms made up of  $L 4 \times 4 \times 1/2$  sections were used to prevent distortion of the cross-section. Internal diaphragms were spaced approximately every 6 m (20 ft) for the Z-connect and every 4.8 m (16 ft) for the K-connect. In addition to internal braces, external diaphragms that were made up of  $L 5 \times 5 \times 1/2$  sections were used to maintain alignment during construction. Solid diaphragms were used at support locations. A top-lateral truss system was fastened to the top flanges to form a quasi-closed box section. Top laterals were WT  $7 \times 21.5$  sections for the Z-connect and WT  $8 \times 33.5$  sections for the K-connect. The concrete deck had a width of 9.1 m (360 in.) for both bridges. Each girder centerline was offset from the bridge centerline by 249

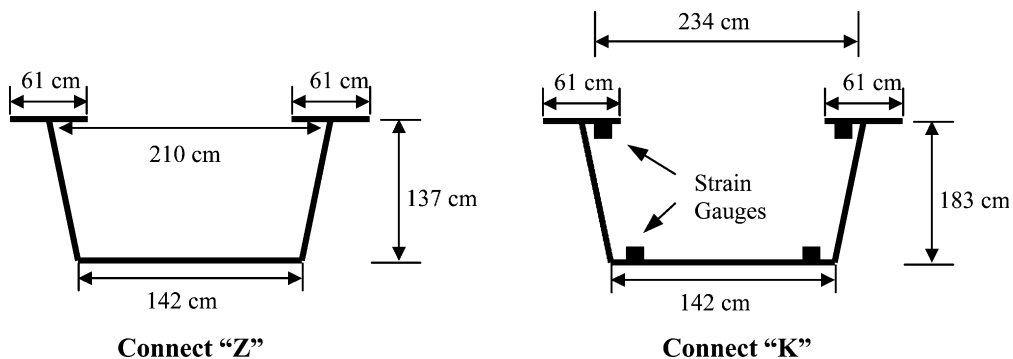


Fig. 5. Dimensions of the girder cross-section.

Table 2  
Plate thickness

Web		Bottom flange		Top flange	
Length m (ft)	Thickness cm (in.)	Length m (ft)	Thickness cm (in.)	Length m (ft)	Thickness cm (in.)
<i>Z-connect plate properties (from 13Z end)</i>					
31 (100.5)	1.27 (0.5)	31 (100.5)	1.90 (0.75)	39 (127)	3.18 (1.25)
30 (99)	1.59 (0.625)	8 (26.5)	3.18 (1.25)	3 (10)	4.44 (1.75)
28 (94)	1.27 (0.5)	3 (10)	3.81 (1.5)	8 (26)	6.98 (2.75)
30 (99)	1.59 (0.625)	8 (26)	5.08 (2.0)	3 (10)	4.44 (1.75)
31 (100.5)	1.27 (0.5)	3 (10)	3.81 (1.5)	44 (147)	3.18 (1.25)
		8 (26.5)	3.18 (1.25)	3 (10)	4.44 (1.75)
		28 (94)	1.90 (0.75)	8 (26)	6.98 (2.75)
		8 (26.5)	3.18 (1.25)	3 (10)	4.44 (1.75)
		3 (10)	3.81 (1.5)	39 (127)	3.18 (1.25)
		8 (26)	5.08 (2.0)		
		3 (10)	3.81 (1.5)		
		8 (26.5)	3.18 (1.25)		
		31 (100.5)	1.90 (0.75)		
$\Sigma = 150$ (493)		$\Sigma = 150$ (493)		$\Sigma = 150$ (493)	
<i>K-connect plate properties (from 17K end)</i>					
41 (134)	1.59 (0.625)	29 (96)	1.90 (0.75)	29 (96)	2.54 (1.0)
34 (113)	1.90 (0.75)	18 (60)	3.81 (1.5)	15 (47)	3.81 (1.5)
26 (84)	1.59 (0.625)	7 (23)	5.08 (2.0)	4 (13)	5.08 (2.0)
34 (113)	1.90 (0.75)	15 (47)	3.81 (1.5)	7 (23)	7.62 (3.0)
41 (134)	1.59 (0.625)	38 (126)	1.90 (0.75)	14 (46)	5.08 (2.0)
		15 (47)	3.81 (1.5)	38 (128)	2.54 (1.0)
		7 (23)	5.08 (2.0)	14 (46)	5.08 (2.0)
		18 (60)	3.81 (1.5)	7 (23)	7.62 (3.0)
		29 (96)	1.90 (0.75)	4 (13)	5.08 (2.0)
				15 (47)	3.81 (1.5)
				29 (96)	2.54 (1.0)
$\Sigma = 176$ (578)		$\Sigma = 176$ (578)		$\Sigma = 176$ (578)	

cm (98 in.) for the Z-connect and 239 cm (94 in.) for the K-connect. Studs having 2.22-cm (7/8 in.) diameter were spaced every 30 cm (12 in.) at both ends of both bridges for a distance of 3 m (10 ft) from the piers. For the remainder of the bridges, studs were spaced at every 60 cm (24 in.). There were three studs per flange over the entire length of each bridge.

#### 4.2. Concrete pouring sequence

After the erection of the steel girders, PMDF were installed between the top flanges of the girders (Fig. 6). Longitudinal and transverse reinforcement (Fig. 6) were then placed on top of the PMDF. The 9.1-m (30-ft) wide concrete deck was placed using a concrete screed. Class S type concrete with a mix design identical to the one used in the shear stud tests discussed earlier was used during the construction. A total of five pours were specified for both bridges. The pour sequence and the length of pours are given in Fig. 4. Both bridges were monitored during the first three pours, and details documenting the start and end times for these pours are given in Table 3.

#### 4.3. Field monitoring

Top-lateral bracing members and cross-sectional stresses were monitored during the pouring sequence. Each instrumented top-lateral WT had two cross-



Fig. 6. Permanent metal deck forms (PMDF) and reinforcement installation.

Table 3  
Start and end times for the first three pours

	Start		End		Duration
<i>Z-connect</i>					
Pour 1	8/31/00	11:40 p.m.	9/1/00	2:20 a.m.	2 h 40 min
Pour 2	9/1/00	3:00 a.m.	9/1/00	5:30 a.m.	2 h 30 min
Pour 3	9/1/00	6:40 a.m.	9/1/00	10:40 a.m.	4 h 0 min
<i>K-connect</i>					
Pour 1	3/13/01	8:39 a.m.	3/13/01	11:10 a.m.	2 h 31 min
Pour 2	3/16/01	12:27 a.m.	3/16/01	2:05 a.m.	1 h 38 min
Pour 3	3/17/01	12:00 a.m.	3/17/01	3:20 a.m.	3 h 20 min

sections gaged for redundancy. The two axial forces for each member were averaged for each time increment.

Top-lateral members of the first two panels at each end of the Z-connect were monitored for both the inner and outer girders (Fig. 4). Cross-sectional stresses were not monitored for the Z-connect. Eight top-lateral members and four cross-sections were instrumented for the K-connect. Six of the instrumented top laterals were located in the first three panels at pier 17K (Fig. 4). The remaining two instrumented laterals were located at panels 18 and 19 of the outer girder (Fig. 4). Cross-sectional stresses were computed from strain gage readings obtained from four different locations along the length of the bridge. Two of the instrumented cross-sections were located in the middle of panels 2 and 3. For these locations, both the inner and outer girder were monitored. The remaining two instrumented cross-sections were located in the middle of panels 18 and 19. For these locations, only the outer girder was monitored. A total of four gauges were placed per girder cross-section. Two of these gauges were placed at the top flanges while the others were placed at the bottom flange (Fig. 5). Gauges were located at 12 cm (5 in.) from the edge of the plates.

#### 4.4. Field monitoring results

This section presents the changes in force and stress levels for the first three pours of both bridges along with the predictions from the software developed specifically for this research (UTrAp). A discussion of the results will be presented in the following sections.

##### 4.4.1. Z-connect

Pour 1 had a length of 20 m (65 ft) and took approximately 2 h and 40 min to complete. This pour started from the 13Z end of the bridge and progressed toward the middle of the span (Fig. 4). In the analysis of the bridge during this phase of construction, no composite action was assumed; therefore, the interface stud stiffness was considered to be 0. The concrete stiffness was also assumed to be 0 because the curing time during this portion of the construction was very short.

The specified deck thickness was 20 cm (8 in.) as measured from the top surface of the PMDF to the top of the concrete deck. Usually, the total amount of concrete poured is greater than the value calculated according to the specified deck thickness. This additional concrete is needed to fill haunches in the corrugated metal deck. In the analysis, a modified constant deck thickness that takes into account the additional concrete was used. For this purpose, the value of the total amount of concrete poured on the Z-connect was obtained from the contractor. From the total concrete volume, a constant deck thickness value was calculated to be 28 cm (11 in.), and this value was used in all analyses related with the Z-connect. A distributed load value of 58.2 kN/m (3.99 k/ft) was applied for each pour segment in order to simulate the forces resulting from the wet concrete. Changes in axial force levels for the instrumented top laterals, along with the analytical predictions, are given in Fig. 7. A detailed discussion of the results is included in the next section.

Pour 2 had a length of 20 m (65 ft). It started from the middle of the span and progressed towards the 16Z end of the bridge (Fig. 4). Two hours and 30 min elapsed during the completion of this pour. Previously poured concrete on segment 1 had cured nearly 4–6 h

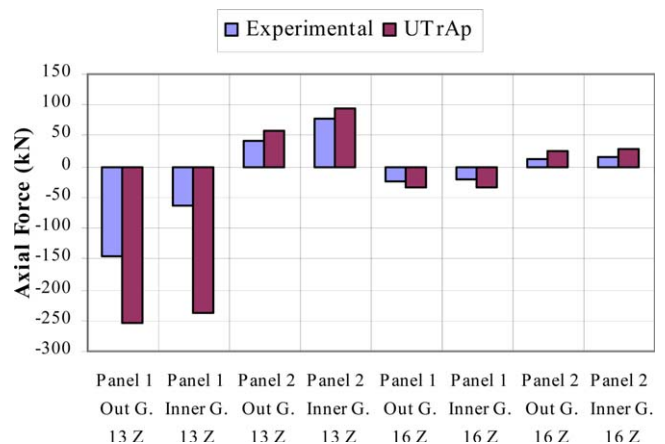


Fig. 7. Change in diagonal force levels due to pour 1 (Z-connect).

when this pour had ended. Although concrete in portion 1 had gained some strength, its value was expected to be very low ( $f'_c < 2$  MPa). Therefore, in the analysis of pour 2, no composite action was assumed for deck segments 1 or 2. A stiffness value of 0 was assigned to the concrete and shear studs of both deck segments. Changes in axial force levels for the instrumented top laterals, along with the analytical predictions, are given in Fig. 8.

Pour 3 had a length of 27 m (90 ft) and was placed at an equal distance from both ends. This pour was completed in 4 h. By the time this pour was finished, concrete on the first segment had cured 6–10 h, and concrete on the second segment cured between 1 and 5 h. In the analysis of pour 3, concrete on segment 1 was assumed to cure for an average period of 8 h. From the laboratory experiments presented earlier, the concrete stiffness for that time period was estimated to be 19.3 GPa (2800 ksi), and the design connector strength at that time period was estimated to be 47 kN (10.6 kips) (Eq. (1)). The load–slip relationship developed earlier (Eq. (2)) revealed that the stud stiffness varies between  $3.75 Q_d$  and  $1.25 Q_d$ . For this case, studs have an initial tangent stiffness of 176 kN/mm (1000 k/in.) and a final secant stiffness of 59 kN/mm (336 k/in.). Because the developed program assumes linear behavior, the non-linear response of the studs has to be approximated using an equivalent elastic stiffness. According to the developed load–slip relationship, the final secant stiffness is one third of the initial tangent stiffness. Therefore, an equivalent elastic secant stiffness of 117 kN/mm (667 k/in.), which is two thirds of the initial stiffness, was selected to represent the stud behavior in segment 1. For segment 2, because a short period of time had elapsed for its curing, it was assumed to act non-compositely. Changes in axial force levels for the instrumented top laterals along with the analytical predictions are given in Fig. 9. For comparison purposes, the analysis results for the case where the

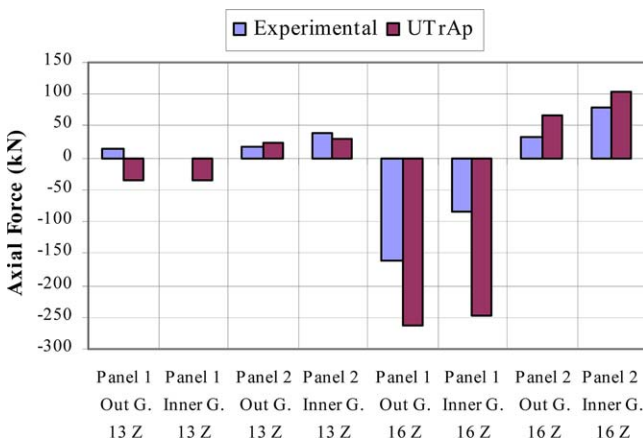


Fig. 8. Change in diagonal force levels due to pour 2 (Z-connect).

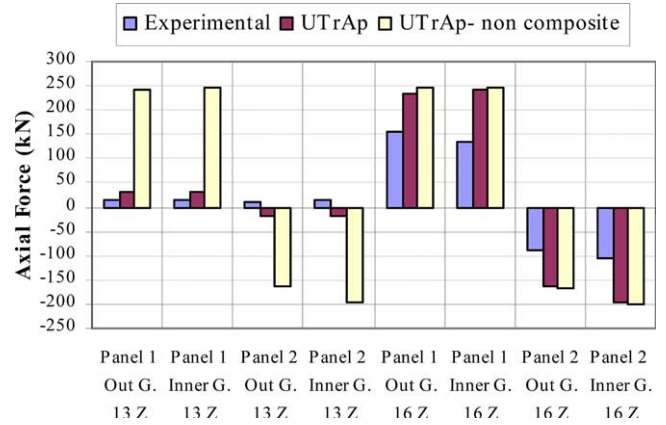


Fig. 9. Change in diagonal force levels due to pour 3 (Z-connect).

entire bridge is assumed to act non-compositely are presented in the same figure.

In order to investigate the validity of the assumptions made regarding the stud stiffness, several additional analyses were performed. In all these analyses, a concrete stiffness of 19.3 GPa (2800 ksi) was used for the first segment, and the stud stiffness value was varied between 0 and 176 kN/mm (1000 k/in.). Analysis results showed that varying the stud stiffness had little effect on the axial force values of the top laterals located near pier 16Z because non-composite action was specified. However, a change in stud stiffness had a significant effect on the axial force values of the top laterals located near pier 13Z. Fig. 10 shows the axial force levels as a function of stud stiffness for the four top-lateral members close to pier 13Z. Analysis results revealed that values of stud stiffness greater than 61 kN/mm (350 k/in.) produce similar results for the top laterals. Therefore, it can be concluded that the assumption of a 117 kN/mm (667 k/in.) value for stud stiffness is reasonable.

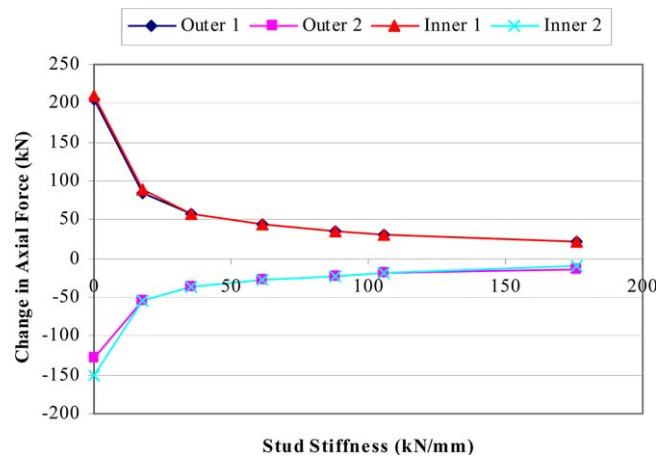


Fig. 10. Effect of stud stiffness on 13Z top-lateral forces (pour 3).

4.4.2. K-connect

Pour 1 had a length of 31 m (100 ft) and took approximately 2 h and 30 min to complete. In the analysis for this phase of construction, the concrete and stud stiffness were considered to be 0. The specified deck thickness for this bridge was 20 cm (8 in.). A constant deck thickness value was calculated to be 25 cm (10 in.) to account for the extra concrete that results when using PMDF, and this value was used in all the analyses related with the K-connect. A distributed load value of 52.9 kN/m (3.625 k/ft) was applied during each pour in order to simulate the forces arising from the wet concrete. Changes in axial force levels and cross-sectional stresses are given in Figs. 11 and 12 along with the analytical predictions. For the cross-sectional stresses, the two strain gage values on the flange were averaged for both the top flange and the bottom flange.

In the figures giving stresses, the following nomenclature is used: Out, outer girder; In, inner

girder; T, top flange; and B, bottom flange. Therefore, Out 3B corresponds to the change in stress at the bottom flange of the outer girder in the middle of panel 3.

Pour 2 had a length of 31 m (100 ft) and was at the opposite end (Pier 20K) of the bridge. One hour and 38 min elapsed during the completion of this pour. Previously poured concrete on portion 1 had cured for 3 days when pour 2 started. From the laboratory experiments and the developed equations, the predicted concrete and average stud stiffness were 28.3 GPa (4100 ksi) and 219 kN/mm (1250 k/in.), respectively, for pour 1. Changes in axial force levels and cross-sectional stresses are given in Figs. 13 and 14 along with the analytical predictions. For comparison purposes, the analysis results for the case where the entire bridge is assumed to act non-compositely are presented in the same figures.

Pour 3 had a length of 40 m (134 ft) and was placed at an equal distance from both ends. This pour was completed in 3 h and 20 min. By the time this pour was

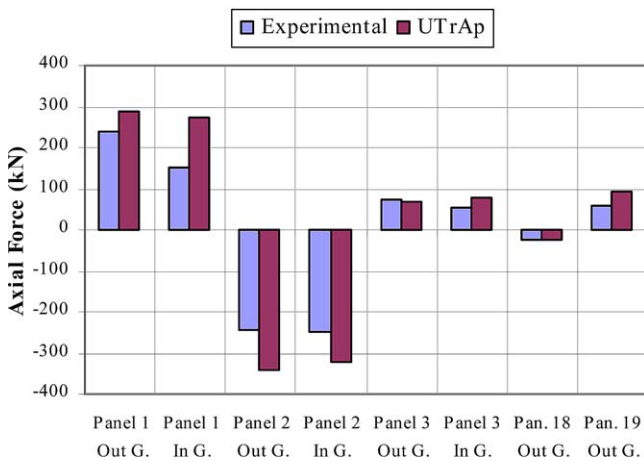


Fig. 11. Change in diagonal force levels due to pour 1 (K-connect).

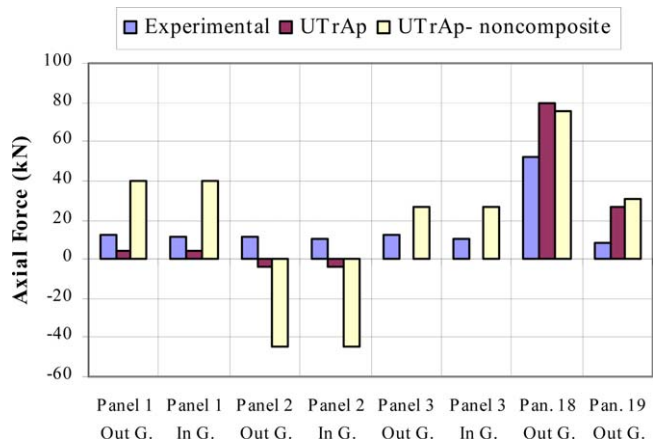


Fig. 13. Change in diagonal force levels due to pour 2 (K-connect).

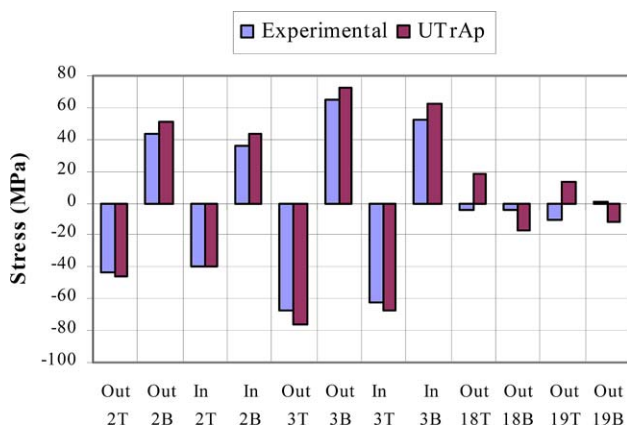


Fig. 12. Change in cross-sectional stresses due to pour 1 (K-connect).

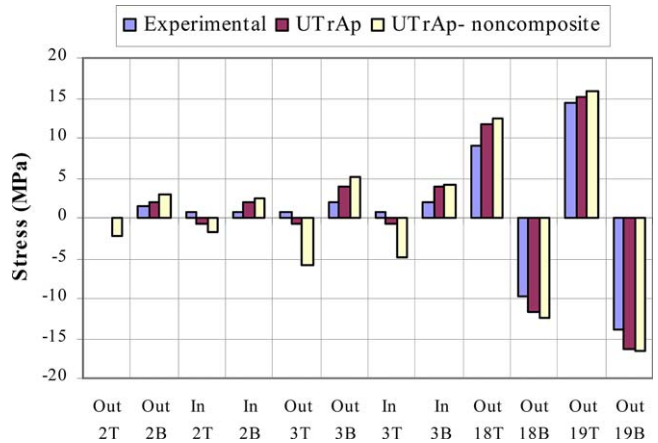


Fig. 14. Change in cross-sectional stresses due to pour 2 (K-connect).

completed, concrete on the first segment had cured for 4 days, and the concrete on the second segment had cured for 1 day. In the analysis, concrete and average stud stiffness were assumed to be 29 GPa (4200 ksi) and 223 kN/mm (1275 k/in.), respectively, for the first segment. The corresponding values for the second segment were 25.5 GPa (3700 ksi) and 175 kN/mm (1000 k/in.). Changes in axial force levels and cross-sectional stresses are given in Figs. 15 and 16 along with the analytical predictions. For comparison purposes, the analysis results for the case where the entire bridge is assumed to act non-compositely are also presented.

4.5. Discussion of analysis results

For both of the bridges, the analytical predictions were in reasonable agreement with the experimental findings. In almost all cases, the analytical predictions were higher than the forces/stresses measured in the field. Top-lateral members and cross-sections that are

closer to the concrete load have higher force and stress changes compared to the ones further away from the pour. For the first pour of the Z-connect, top-lateral members close to the 13Z end pick up higher forces in comparison to the ones near the 16Z end. The opposite is true for the second pour. For the third pour, if no composite action is assumed, force changes in the 13Z and 16Z top laterals should be identical because the bridge is perfectly symmetric. However, Fig. 7 shows that the 13Z top laterals take much less force relative to the 16Z top laterals. This observation indicates that partial composite action is developing during the third pour, and the early-age concrete on the first segment is increasing the stiffness of the cross-section. Additional study to determine the large difference between measured and predicted values for the inner girder 13Z top lateral 1 was inconclusive.

The prediction of top-lateral member forces for the K-connect are better than the ones for the Z-connect. In addition, the prediction of stresses is better than the ones for the top-lateral member forces. The noted discrepancies can be attributed to several shortcomings of the modeling assumptions incorporated in the developed software. These shortcomings will be explained in the following section.

5. Additional analyses

The effects of the modeling shortcomings on the results were investigated further. The study was carried out by making use of a commercially available, general purpose finite element program, ABAQUS [8]. In the following sections, details of the modeling with ABAQUS and a discussion of various shortcomings of UTrAp are presented.

5.1. Finite element model used in ABAQUS

The same mesh density used in UTrAp was used for modeling the bridges in ABAQUS. Eight-node quadratic shell elements with reduced integration (S8R5) were used to model the top and bottom flanges, webs and pier diaphragms. Instead of shell elements, three-dimensional, 20-node quadratic bricks (C3D20) were used to model the concrete deck. The use of brick elements has the advantage of modeling a tapered deck thickness profile. One and 20 brick elements were used along the thickness and width of the deck, respectively. All bracing members were modeled with two-node linear beam elements (B31). Spring elements were placed between the top flange and concrete deck to simulate the studs.

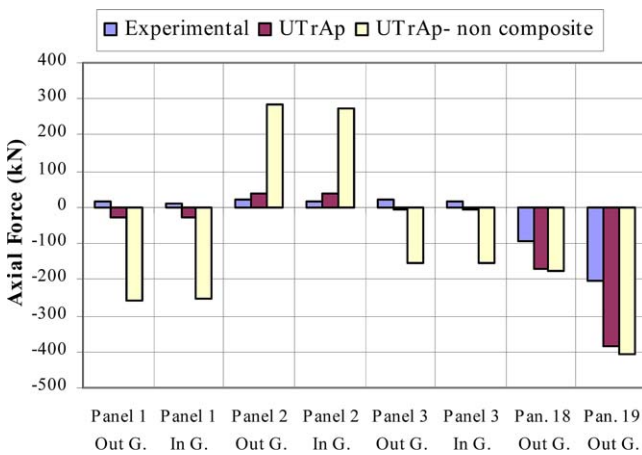


Fig. 15. Change in diagonal force levels due to pour 3 (K-connect).

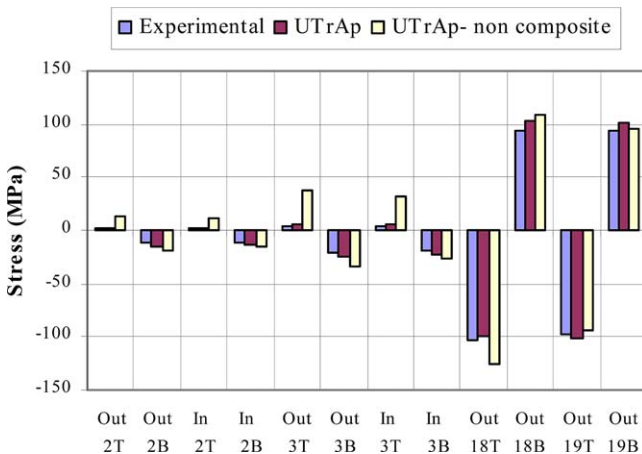


Fig. 16. Change in cross-sectional stresses due to pour 3 (K-connect).

## 5.2. Shortcomings of the UTrAp model

### 5.2.1. Superelevation

UTrAp forms the model of the bridge without accounting for horizontal superelevation. In reality, however, the bridges studied under this research project have moderate levels of horizontal superelevation. For example, the Z-connect has a 6% superelevation. If there is no superelevation, then forces due to concrete weight are applied vertically to the bridge. In the case of superelevation, concrete weight has a horizontal component that acts on the bridge. This horizontal component produces a constant torque along the length, which counteracts the forces due to the vertical component. In general, including superelevation into the model reduces the level of forces calculated for top-lateral members.

### 5.2.2. Deck thickness profile

During the design of these bridges, a constant concrete deck thickness is specified. Due to construction limitations, it is very difficult to place concrete evenly on the PMDF. Therefore, in some cases, the deck thickness profile becomes non-uniform. This kind of non-uniformity was not included in the finite element model in UTrAp because it is not easily predicted at the design stage. For the bridges mentioned in this study, the thickness of the deck along the width and length of the bridge were measured by TxDOT engineers during construction. The measurements revealed that the poured deck had a fairly uniform cross-section for the K-connect and had a tapered cross-section for the Z-connect. The thickness of the deck reduced gradually from the inner portion of the bridge to the outer portion (from 31.5 cm (12.4 in.) to 24.3 cm (9.6 in.)) for connect Z. Placing concrete unevenly has effects on the measured forces. In this case, placing more concrete on the inner girder compared to the outer girder causes a torque along the length of the bridge that counteracts the torsional forces due to the curved geometry of the bridge. The sensitivity of the predicted forces to deck thickness profile will be discussed later.

### 5.2.3. Support movements

In the software developed, no vertical movement is allowed at the support locations. Under field conditions, however, some vertical support movement is expected. During the construction of these bridges, elastomeric bridge bearings were used at the support locations. Because bearings do not possess infinite compressive and rotational stiffness, some degree of movement should be expected at the piers. The sensitivity of the predicted forces to support movements will be addressed below.

### 5.2.4. Permanent metal deck forms

As mentioned earlier, PMDF were placed atop the girders to act as a formwork for the concrete deck. In current practice, PMDF are attached to a thin angle section that is welded to the top flanges. This kind of attachment detail is very weak due to the low stiffness of the angle section. Currently, in a related research project at the University of Texas, different attachment details are under investigation [9]. One of the details studied was the direct attachment of PMDF to the top flanges with power-actuated fasteners. This detail was also implemented on the instrumented bridges. The first three panels at each end of the outer girder for the Z-connect, and the first three panels from 17K of both the inner and outer girder for the K-connect, were covered with PMDF attached with power-actuated fasteners. Regardless of the attachment detail, the PMDF stiffens the cross-section to some degree. At the present time, however, there is no information on quantifying the level of stiffness gain due to the attachment of PMDF to the top flanges. Therefore, the effects of PMDF are excluded in all finite element analyses.

### 5.2.5. Connection details

In the Z- and K-connects, the top flange bracing members were bolted, not welded, to the top flanges. Bolted shear connections are more flexible in comparison to rigid welded connections. In the bridges investigated for this research, the bolts were specified to be fully torqued in the shop using the turn-of-the-nut tightening method [10]. During construction, however, bolts are frequently loosened in the field to provide some flexibility for erectors completing the girder field splices. In all the finite element analyses, rigid connections were assumed. Bolted tension and shear connections were also used to connect the external diaphragms to the girders [5]. Due to the flexibility of these joints, the force distribution between the girders might be different than the calculated values which assumed rigidly connected elements.

### 5.2.6. Eccentrically loaded top-lateral members

As explained in the previous paragraph, bolted connections were used to fasten the top-lateral WT members to the top flanges. In all the analyses presented thus far, top-lateral members were modeled with truss elements. This type of modeling assumes that the top-lateral members are concentrically loaded. However, in reality, these members are eccentrically loaded due to the attachment detail. Eccentric loading produces equal and opposite end moments on the member which result in a more flexible behavior. The effect of eccentrically loaded brace members can be studied by modifying the area of the top-lateral members so as to reduce the effective stiffness of the member due to axial loads. A modified area can be calculated by including the

additional axial deformation of the elements caused by bending of the members. The axial deformation due to concentric loading ( $\Delta_a$ ) can be expressed as  $\Delta_a = PL/EA$  where,  $P$  is the axial force,  $L$  is the length of the member,  $A$  is the cross-sectional area, and  $E$  is the modulus of elasticity. The additional axial deformation caused by eccentric loading ( $\Delta_b$ ) can be expressed as  $\Delta_b = PL e^2/2EI$  if equal and opposite end moments are assumed. In the previous formula,  $e$  is the eccentricity, and  $I$  is the moment of inertia.

If an eccentricity of 49 mm (1.93 in.) (33 mm depth of neutral axis plus 16 mm half-thickness of the top plate) is considered for the Z-connect WT members, a modified area of 26.5 cm<sup>2</sup> (4.1 in.<sup>2</sup>— 65% of original area) should be used in the analysis. The sensitivity of the predicted forces to eccentric loading will be discussed below.

### 5.3. Sensitivity study

In order to investigate the effects of superelevation, deck thickness profile, and eccentric loading, three additional analyses for the Z-connect were performed using ABAQUS. In the first analysis, pour 1 was simulated by incorporating the superelevation into the model. In the second analysis, both superelevation and the tapered deck thickness profile were included. In the third analysis, all three details (superelevation, deck thickness profile and eccentric loading) were included. Fig. 17 presents the results for all of these analyses together with the experimental findings presented earlier. It is evident that including the superelevation, tapered deck thickness profile, and eccentric loading produces estimates that are closer to the experimental findings. Axial forces on the braces tend to decrease by 9% on average by including superelevation in the

model. Forces are reduced further by 17% on average by including the tapered thickness profile and 7% on average by including the eccentric loading.

Another issue mentioned earlier was the effect of support movements. In order to investigate this effect, a support rotation of 0.008 rad was applied to one of the end supports of the Z-connect. This value corresponds to a 2.54 cm (1 in.) upward movement for the outer girder and 2.54 cm (1 in.) downward movement for the inner girder. Analysis results revealed that for this case, the axial forces for the first and second panel top laterals changed by 93.4 kN (21 kips). These analysis results indicate that the support movements may have significant effects on the measured top-lateral forces.

In general, results from the finite element analysis with superelevation, tapered deck thickness profile, and eccentric loading were closer to the field measurements than those predicted with UTrAp. Some discrepancies were still not resolved with these modifications, and the noted variation in the predicted and measured results could be attributable to, for example, the level of detail in modeling the effects of the PMDF and the bolted connections. Because these other effects are difficult to quantify, no further analyses were conducted. While it may be possible to improve analytical results by accounting for such features as superelevation, the developed software provides reasonable and conservative estimates for design.

## 6. Conclusions

The findings of a three-phase research study on the behavior of curved, trapezoidal, steel box-girders during construction were presented. The first two phases

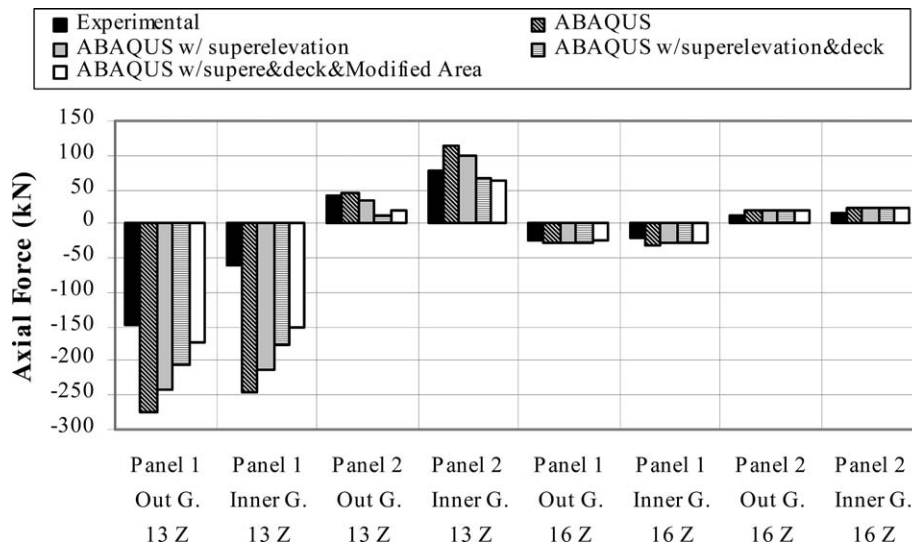


Fig. 17. Sensitivity study on Z-connect.

focused on the investigation of steel–concrete interface behavior at early concrete ages and the development of an easy-to-use computer program to incorporate the semi-cured concrete deck behavior into an analysis routine. In the last phase, two curved bridges were monitored during the concrete pouring sequence. The field results were compared with the predictions obtained using the developed software. The following can be concluded from this study:

- The experimental findings clearly reveal that composite action occurs at very early concrete ages. For the Z-connect, the effects of composite action were observed as early as 8 h after the initial pour.
- The analytical predictions were in reasonable agreement with the experimental findings. In general, the program was capable of generating acceptable results for cases where there was no composite action. For cases with early composite action, the differences in predicted and measured quantities were much higher. Based on results from connect-K, the predictions for girder stresses were much better than those for top-lateral forces. Overall, the analytical predictions are sufficient for a conservative design.
- Sensitivity studies revealed that including super-elevation, a tapered deck thickness profile and eccentric loading of braces into the analysis model improves the quality of the analysis results. In almost all cases, the analytical predictions were higher than the forces/stresses measured in the field. The reason for these discrepancies was the lack of knowledge of the effects of some details that were not included in the analytical model. These details include the modeling of PMDF and flexible connections as well as support movements. Future research should concentrate on the sensitivity of the analysis results to these details.
- The concept of early composite action will lead to a better understanding of bridge behavior. The use of this concept, together with the developed software, will yield more accurate and cost effective designs. Information contained herein can be used to investi-

gate the potential benefits of early composite action in reducing the costs associated with these structural systems. Reliance upon early composite action in design will yield a reduction in the magnitude of top flange diagonal forces and in the number of bracing members required for acceptable structural performance.

### Acknowledgements

This research was a part of a larger research project supported by a contract from the Texas Department of Transportation (TxDOT Project No. 1898). The conclusions drawn in this paper are the opinions of the authors and do not necessarily reflect the opinions of the sponsor. The writers extend special thanks to Professor Joseph Yura for his guidance, as well as Ben Chaplak, Matthew Memberg, and Brian Chen, for their help in the field studies.

### References

- [1] Kollbrunner CF, Basler K. Torsion in structures—an engineering approach. New York: Springer-Verlag; 1969.
- [2] Sennah KM, Kennedy JB. State-of-the-art in design of curved box-girder bridges. *ASCE Journal of Bridge Engineering* 2001;6(3):159–67.
- [3] Holt J. TxDOT design engineer. Personal contacts; 2001.
- [4] Fan Z. Field and computational studies of steel trapezoidal box-girder bridges. PhD dissertation, University of Houston; 1999.
- [5] Cheplak BA. Field measurements of intermediate external diaphragms on a trapezoidal steel box-girder bridge. Thesis, University of Texas at Austin; 2001.
- [6] Topkaya C. Behavior of curved steel trapezoidal box-girders during construction. PhD dissertation, University of Texas at Austin, Texas; 2002.
- [7] Viest IM, Colaco JP, Furlong RW, Griffis LG, Leon RT, Wyllie LA. Composite construction design for buildings. New York: McGraw-Hill; 1997.
- [8] ABAQUS. Standard user's manual. Hibbit, Karlsson, and Sorensen, Inc., USA; 1997.
- [9] Chen BS. Top-lateral bracing systems for trapezoidal steel box-girder bridges. PhD dissertation, University of Texas at Austin; 2002.
- [10] AISC. Manual of steel construction—load and resistance factor design. 2nd ed. Chicago; 1994.